Mecánica Computacional Vol. XXIII, pp. 1807-1822
G.Buscaglia, E.Dari, O.Zamonsky (Eds.)
Bariloche, Argentina, November 2004

ERROR ANALYSIS AND VALIDATION OF STRATOSPHERIC OZONE PROFILES

S. Enrique Puliafito*, Carlos M. Puliafito,

Universidad de Mendoza
Arístides Villanueva 773 5500, Mendoza – Argentina.
Tel ++54 (261) 4202017 , e-mail: epuliafito@frm.utn.edu.ar
*Research member of CONICET, now at Universidad Tecnológica Nacional

Keywords: Error analysis, remote sensing, stratospheric ozone profiles, validation

Abstract: *From 1993 to 2000, the Institute for Environmental Studies (IEMA) depending of the University of Mendoza, carried out ground-based stratospheric ozone measurements by means of millimetre wave radiometry (Project TROPWA). In this paper we present a complete theoretical study necessary to qualify the uncertainties in the retrieval process. This type of error analysis is often used to characterize any remote sensing experiment. To evaluate and validate the quality of the obtained TROPWA stratospheric ozone profiles, we also performed a comparative study using the ozone profiles measured by the HALOE experiment. This study includes a comparison of individual profiles and of seasonal averages from 1993 to 2000. Given the coarser height resolution of the retrieved ozone profiles from microwave ground based instrument, compared to those obtained from the solar occultation technique, the HALOE profiles were averaged by convolving them with the averaging kernels of the TROPWA retrieval process. This error analysis and the comparison tests allowed us to evaluate and characterize the retrieval of our instrument. It can be seen that from 20 to 40 km the TROPWA instrument is able to retrieve ozone profiles with absolute errors varying from 10 to 20 %, and relative errors less than 5%, with a height resolution (FWHM) that varies from 5 to 11 km depending on the altitude. The seasonal variations show consistent patterns but having TROPWA measurements a systematic lower peak value of about 0.5 to 0.7 ppmv. The mayor discrepancies between both set of profiles occurs in the period of May-June with values varying around +8 to –10% (+0.4 to –0.8 ppmv). This difference is partially due to the coarser height resolution of our instrument.*

1 INTRODUCTION

The Institute for Environmental Studies (IEMA), University of Mendoza has performed ground based measurements of tropospheric water vapour and stratospheric ozone, by means of millimetre wave radiometry, from 1993 to year 2000, according to Table 1, from Mendoza, Argentina. The Tropospheric Water Vapour and Stratospheric Ozone (TROPWA) Project has three millimetre wave radiometers working at different frequencies: 21.8 GHz, 22.2 GHz, 31.5 GHz, 92 GHz, and 142 GHz for water vapour, water vapour continuum and ozone respectively. From these data it is possible to retrieve stratospheric ozone profiles from approximately 20 to 40 km altitude with an altitude resolution ranging from 5 to 11 km, depending on the altitude and with a minimal temporal resolution of one hour.

In this paper we will present the error analysis typically used to characterize remote sensing instruments, such as the TROPWA ozone instrument. To test this study we used a data set of ozone profiles from the Halogen Occultation Experiment (HALOE) on board the Upper Atmosphere Research Satellite (UARS). The HALOE Instrument uses solar occultation technique and has been taking data nearly continuously since 1991. It measures vertical profiles of O_3, HCl, HF, CH_4, H_2O, NO, NO_2, aerosol extinction, and temperature versus pressure. HALOE sweeps from 80 S to 80 N in latitude approximately every 30 days. Russell[1] gives a complete description of this instrument and operation, and Bruhl[2] presents the HALOE error analysis study.

Table 1: Measurement periods and sites.

TROPWA	Date			Site			
21-nov-93	22-nov-93	23-nov-93	24-nov-93	25-nov-93	26-nov-93		Puente del Inca
15-dic-93	25-abr-94	1-jul-94	3-aug-94	4-aug-94	5-aug-94		Benegas
8-nov-94	9-nov-94	10-nov-94	11-nov-94				Puente del Inca
12-jun-95	13-jun-95	14-jun-95	15-jun-95	16-jun-95	22-sep-95	26-sep-95	Uspallata
10-abr-95	18-oct-95	19-oct-95	20-oct-95	19-mar-96	11-jun-96	23-aug-96	Benegas
1-oct-96	13-aug-97	15-sep-97	16-sep-97	17-sep-97	8-oct-97	9-oct-97	Benegas
10-oct-97	5-may-98	7-may-98	8-may-98	11-may-98	12-may-98	29-jul-98	Benegas
31-jul-98	3-aug-98	4-aug-98	5-aug-98	26-aug-98	28-aug-98	31-aug-98	Benegas
10-sep-98	28-oct-98	29-oct-98	5-may-99	9-jun-99	7-jul-99	26-jul-99	Benegas
28-mar-00	29-mar-00						Benegas

2 MATERIALS AND METHOD

2.1 Instrumentation

Remote sensing of ozone at millimetre wavelength is an adequate technique to measure the vertical ozone distribution at the stratosphere and the mesosphere. The main advantage over other techniques is given by the fact that measurements can be taken continuously day and night because the technique does not require any external source of radiation. In addition it

can measure under nearly all weather conditions. Only if the water vapour content is large or in presence of rain, ozone profiles are difficult to obtain.

A radiometer is a heterodyne radio frequency receiver which is tuned at the frequency of a rotational (or vibrational) transition of a trace gas.The radiation emitted from different altitudes suffers a pressure broadening proportional to the pressure in that altitude. Thus by measuring the spectral line width of the radiation received at ground it is possible to derive the altitude from where the radiation is coming from. If the radiation is emitted from more than one altitude you will observe basically the sum of all the contributions from different altitudes and the task of the inversion is to decompose this sum into the single contributions. These effects are considered in the radiative transfer equation[3]. The brightness temperature measurement is then very sensitive to the ozone concentration at different altitudes. Finally, if we know the temperature and pressure profile of the atmosphere, it is possible to retrieve the vertical ozone distribution through mathematical inverse algorithms.

The measured radiation for an upward looking ground-based radiometer expressed in terms of brightness temperature is given by the radiative transfer equation being s_B the ground level and s_A the farthest atmospheric upper layer:

$$T_B(f) = T_A(f) e^{-\int_{s_A}^{s_B} \alpha(f,s)\,ds} + \int_{S_A}^{S_B} T(s)\, y(f,s)\, \alpha(f,s)\, e^{-\int_{s_A}^{s} \alpha(f,s')\,ds'}\, ds \qquad (1)$$

where $y(f,s) = \dfrac{x}{e^x - 1}$, and $x = hf / kT$, $\alpha(f,s) = \alpha(T(s), P(s), VMR, f,$ *spectral parameters):* absorption coefficient [dB/km], *P(s)*: pressure [*mbar*] , *T(s)*: Absolute temperature [K], *VMR*: volume mixing ratio [ppm: parts per million], f : frequency [Hz], s : position along the line of sight [m].

In order to convert the output of the instrument (pure voltages or counts) into brightness temperature, the instrument is calibrated against known brightness temperatures, i.e. a hot load (T_{BH} = 292 K) and a cold load (T_{BC} = 74.6 K). This calibration process is also used to reduce errors introduced by gain drifts in the amplifier chain within the instrument.

The radiometric sensitivity or radiometric resolution ΔT is defined as the smallest change in the received T_B that can be detected by the radiometric output and can be written as:

$$\Delta T = \frac{T_{SYS}}{\sqrt{\Delta f\ \tau}} \qquad (2)$$

where, ΔT is the temperature resolution [K], T_{SYS} is the radiometer noise temperature [K], Δf is the radiometer bandwidth [Hz], and τ is the integration time [s]. Equation (2) is completely valid if the bandwidth is sufficiently small compared to the centre frequency[4], which is our case.

The output signal coming from the 142 GHz ozone total power radiometer is introduced to the backend, i.e. a filterbank spectrometer, which analyses the spectral components of the

intermediate frequency band (IF). The IF was selected in 3.7 GHz and has a bandwidth of ± 600 MHz. The filter bank spectrometer has nine channels with different bandwidths, and it was recently extended to 19 channels. The data are integrated and recorded in a personal computer, generally, in files of 10 minutes long. Hence the real integration time corresponding to the ozone measurement is of 200 seconds. Table 2 indicates the bandwidth, offset frequency, measured noise temperature and the resulting radiometric resolution ΔT for each channel of the spectrometer. Another important error source for the profile retrieval, is the so called baseline structure, which appear as an impedance mismatch between the antenna and mixer, in the front-end of the radiometer, creating a standing wave of several 100 MHz period.

In a ground-based measurement, the radiometer not only receives the brightness temperature information from the spectral line, but also from a tropospheric continuum contribution. The tropospheric water vapour represents one of the most important constituents considered in the tropospheric contribution due to its high opacity, producing an important attenuation. Thus, a tropospheric correction to the measurements must be achieved, i.e. by using the information either from the farthest channel from the ozone centre line, or in our project also from the 92 GHz water vapour radiometer. We also study the tropospheric transmission, using three years of daily radiosounding launched by the Argentine National Weather Service at the Mendoza Airport (years 1993 to 1995). Using the radiosounding profiles we performed a climatological monthly tropospheric profiles of pressure, temperature and water vapour density. Figure 1 shows a measured and corrected spectrum. A major description of the 142 GHz radiometer-spectrometer hardware has been described by Puliafito[5].

Table 2: Filterbank characteristics

Channel Number	Offset Freq. [MHz]	Bandwidth [MHz]	Typical noise temperature @ 200 s int. time	ΔT [K]
0	-350	100	14000	0.06
1	-250	100	15800	0.06
2	-140	40	19800	0.13
3	-60	40	20700	0.13
4	0	2	22400	0.20
5	60	40	18400	0.12
6	140	40	19500	0.13
7	250	100	18300	0.08
8	350	100	21200	0.09

Ozone line center frequency @ 142.175040 GHz

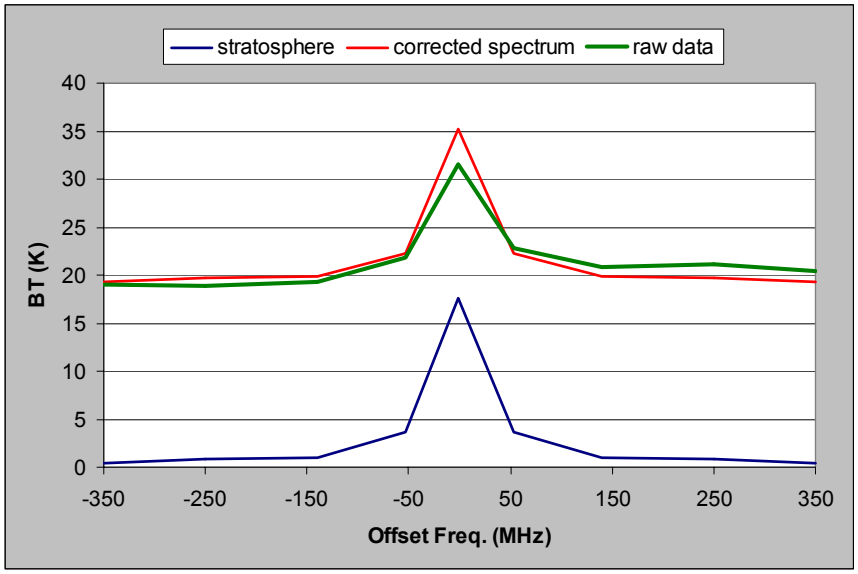

Figure 1: Measured spectrum during Nov. 1993: (a) green line: rwa data as they are measured by the radiometer; (b) red line: Corrected spectrum through baseline removal; C) blue line: Stratospheric spectrum, calculated after tropospheric water vapor removal.

2.2 Data retrieval

If the temperature and the pressure profile of the atmosphere are known, in eq. (1), it is possible to determine the volume mixing ratio of the trace gas from the measured brightness temperature as a function of the frequency (T_B *(f)*). This retrieval procedure is known as *brightness temperature inversion*. We will now briefly describe the mathematical method, which is used to retrieve mixing ratio profiles of a given atmospheric gas. The general remote sensing equation can be written in schematic matrix form, according to Rodgers[6], as

$$\mathbf{y} = \mathbf{F(x,b)} + \boldsymbol{\varepsilon}_y \tag{3}$$

where **y** is the measurement vector, **F(x,b)** is the forward model, **b** is a set of parameters used in the forward model (e.g. line strength, collisional broadening and atmospheric temperature) which must be estimated, $\boldsymbol{\varepsilon}_y$ is the measurement error with covariances $\mathbf{S}_E$, and **x** is the profile to be inferred from the measurement. The retrieved profile $\hat{x}$ can be generally expressed as[7]:

$$\hat{\mathbf{x}} = \mathbf{R}(\mathbf{y}, \hat{\mathbf{b}}, \mathbf{c}, \boldsymbol{\varepsilon}) = \mathbf{T}(\mathbf{x}, \hat{\mathbf{b}}, \mathbf{c}, \boldsymbol{\varepsilon}) \tag{4}$$

where **R** represents the retrieval algorithm, $\hat{\mathbf{b}}$ is our best guess of the forward parameters, and **c** represent any other parameter used in the inverse model, for example a-priori profiles, etc. Also it can be written as a transfer function **T**, relating the retrieved profile with the true

profile **x**. The problem of retrieving constituent mixing ratio profiles from microwave spectral line measurements is, in general, non-linear and therefore in these retrieval problems non-linear techniques need to be employed. In such techniques the weighting functions or kernels are first calculated based on a-priori profiles and then iterated in the solution algorithm[7]. Equation (3) can be linearlised about the a priori value of **x**, $\boldsymbol{x_a}$, and the corresponding estimate of **y** from the forward model, as

$$\mathbf{y} = \hat{\mathbf{y}}(\mathbf{x_a}) + \mathbf{K}(\mathbf{x} - \mathbf{x_a}) \tag{5}$$

where $\hat{\mathbf{y}} = (\mathbf{x_a}) = \mathbf{F}(\mathbf{x_a}, \mathbf{b})$. **K** is the measurement kernel or weighting functions defined as

$$\mathbf{K} = \frac{\partial \mathbf{F}(\mathbf{x},\mathbf{b})}{\partial \mathbf{x}} \tag{6}$$

The optimal estimation inversion techniques has been described by Rodgers[6,8]:

$$\hat{\mathbf{x}} = \mathbf{x_a} + \mathbf{S_X}\mathbf{K}^{\mathbf{T}}(\mathbf{K}\mathbf{S_X}\mathbf{K}^{\mathbf{T}} + \mathbf{S_E})^{-1}(\mathbf{y} - \mathbf{K}\mathbf{x_a}) \tag{7}$$

where $\mathbf{S_X}$ is the covariance matrix of the a priori profile $\mathbf{x_a}$ and $\mathbf{S_E}$ is the covariance matrix of the measurement error. Several other retrieval methods have been compared by Puliafito[7], including the error analysis of each method.

2.3 Error analysis

An important question in every remote sensing technique is to qualify the uncertainties due to different error sources, and how they affect the retrieved profile. Several ways of qualifying these uncertainties have been proposed[6,7,8]. The total error covariance in the inversion process can be expressed as the sum of all different contributions, that is,

$$\mathbf{S_{TOT}} = \mathbf{S_N} + \mathbf{S_M} + \mathbf{S_S} \tag{8}$$

where $\mathbf{S_M}$ is the measurement error and $\mathbf{S_S}$ is the forward model error. $\mathbf{S_N}$, the null-space error, characterizes the spatial resolution in the retrieval process mainly due to the instrument geometry, the mathematical calculations, and the used a-priori information. It is defined as:

$$\mathbf{S_N} = (\mathbf{A}-\mathbf{I})\mathbf{S_X}(\mathbf{A}-\mathbf{I})^T \tag{9}$$

where ***A*** is the so-called averaging kernel matrix, which considers the sensitivity of the retrieval to the true profile, ***I*** is the identity matrix and $\mathbf{S_X}$ is the estimated covariance of the unknown profile *x*.

$$\mathbf{A} = \frac{\partial T}{\partial \mathbf{x}} = \frac{\partial \hat{x}}{\partial \mathbf{x}} = \mathbf{S_x}\mathbf{K}^{\mathbf{T}}(\mathbf{K}\mathbf{S}_X\mathbf{K}^{\mathbf{T}} + \mathbf{S}_E)^{-1}\mathbf{K} \tag{10}$$

The covariance matrix for the measurement error can be calculated using the expression:

$$\mathbf{S_M} = \mathbf{D}\,\mathbf{S}_E\,\mathbf{D}^{\mathbf{T}} \tag{11}$$

where $\mathbf{S}_E$ is the covariance matrix describing the brightness temperature (measurement) error, and **D** is called the contribution function, which defines the sensitivity of the retrieved profile, $\hat{\boldsymbol{x}}$, to the measurements or to the noise, $\boldsymbol{y}$, and can be expressed as:

$$\mathbf{D} = \frac{\partial T}{\partial \varepsilon} = \frac{\partial \bar{\mathbf{x}}}{\partial \mathbf{y}} = \mathbf{S}_X \mathbf{K}^{\mathbf{T}} (\mathbf{K}\mathbf{S}_X \mathbf{K}^{\mathbf{T}} + \mathbf{S}_E)^{-1} \tag{12}$$

Additionally, uncertainties in determining the tropospheric contribution due to meteorological variability, or residual baseline structure in the measured spectra can be treated as a measurement error $\mathbf{S}_M$ (eq. 11), and thus it can be included the $\mathbf{S}_E$ covariance matrix. In this way, $\mathbf{S}_E$ includes the measurement error itself, the baseline residual, and the uncertainty produced by the tropospheric attenuation[9]. Generally, for ground based measurements, the higher the water vapour concentration is, the larger the difficulty or uncertainty in retrieving ozone profile.

By integrating longer, it is possible to reduce measurement noise variances ($\mathbf{S}_E$), up to a certain point where no longer integration does improve the spectrum. Especially since the forward model uncertainties, the tropospheric uncertainties and the baseline structure can not be removed by integration time. As the averaging kernels and the contribution matrices are function of both covariances $\mathbf{S_X}$ and $\mathbf{S}_E$, reducing $\mathbf{S}_E$ along does not necessarily reduce $\mathbf{S}_M$, since $\mathbf{S_X}$ also contributes to **D** (eq. 12). However, reducing $\mathbf{S}_E$ will indirectly improve **A** (eq. 10) and thus may obtain some improvement in the height resolution.
The forward model error covariance is given by:

$$\mathbf{S_S} = \mathbf{D}\,\mathbf{K}_B\,\mathbf{S}_B\,\mathbf{K}_B^{\mathbf{T}}\,\mathbf{D}^{\mathbf{T}} \tag{13}$$

D is again the contribution function, and $\mathbf{K}_B$ considers the sensitivity of the measurements to the forward model parameters **b** (spectral parameters). $\mathbf{S}_B$ is the forward model parameter error covariance.

The variability of the retrieved profile from the measurement errors ($\mathbf{S_M}$) contributes to the relative errors. Instead the $\mathbf{S_N}$, and $\mathbf{S_S}$ are responsible for the absolute estimation of the retrieved information. If we compare one to another retrieved profile only the relative error should be considered. However, if a profile from different experiments or techniques is intercompared (validated), then it is necessary to use the absolute errors, by convolving the averaging kernels of the lower resolution method with the high-resolution profile. Finally, in a retrieved height profile, the error bars at each altitude are then given by the square root of the diagonal elements of $\mathbf{S}_{TOT}$ (eq. 8).

2.4 Validation with other techniques

Figure 2 illustrates the averaging kernels (matrix **A**, eq. 10) versus height. This picture indicates the degree of accuracy when retrieving a perturbation for a given height. Each curve represent a row in the A matrix, and gives an indication of the altitude resolution. Table 3 shows this resolution measured as full width at half maximum (FWHM) of the kernel. For example, the line indicated with triangles, corresponds to a perturbation or a spike of 1 ppmv and 9 km FWHM, at 27 km. These lines demonstrate how a perturbation in one height affects all other heights in the inversion process.

Table 3: Height resolution calculated from the averaging kernels, measured as full width at half maximum

Peak	17 km	20 km	23 km	26 km	29 km	32 km	35 km	38 km	41 km	44 km
FWHM	5 km	6 km	8 km	9 km	10 km	12 km	12 km	12 km	12 km	12 km

Rodgers and Connors[10], present a detailed discussion of the use of the averaging kernels and how this information may be used to determine the influence of the selected a-priori profile into the retrieval. Furthermore this paper also presents the methodology for comparing retrieval coming form different instruments, especially with different height resolution. This validation process is also clearly presented by Nedoluha [11]. Following these excellent papers, it can be seen how the retrieved profile $\hat{x}$ is related to the true profile x and the a priori profile $\boldsymbol{x}_a$ by

$$\hat{\mathbf{x}} - \mathbf{x}_a = \mathbf{A}(\mathbf{x} - \mathbf{x}_a) + \mathbf{D}\boldsymbol{\varepsilon}_y \tag{14}$$

where **A** are the averaging kernels. Further arrangements may lead to:

$$\hat{\mathbf{x}} - \mathbf{x} = (\mathbf{A} - \mathbf{I})(\mathbf{x} - \mathbf{x}_a) + \mathbf{D}\boldsymbol{\varepsilon}_y \tag{15}$$

where the first term **(A-I)(x-xa*)*** can be defined as smoothing error.

Equation (14) can be rewritten to determine the effect of the a priori on the retrieval process:

$$\hat{\mathbf{x}} = \mathbf{A}\mathbf{x} + (\mathbf{I} - \mathbf{A})\mathbf{x}_a \tag{16}$$

Here we see that if **A = I** (**I*:*** identity matrix) the retrieved profile will recover the true profile; otherwise a proportion of the a priori will be passed to the retrieved profile through $(\mathbf{I}-\mathbf{A})\mathbf{x}_a$. Figure 3 show the influence of the a priori profile for the TROPWA configuration. It can be seen that from 20 to 40 km, the contribution of the selected a-priori profile is less than 30%, all other altitudes the dependence is much higher. At present, a new spectrometer with narrower filters closer to the centre line is being tested, thus allowing the retrieval of better information at higher altitudes.

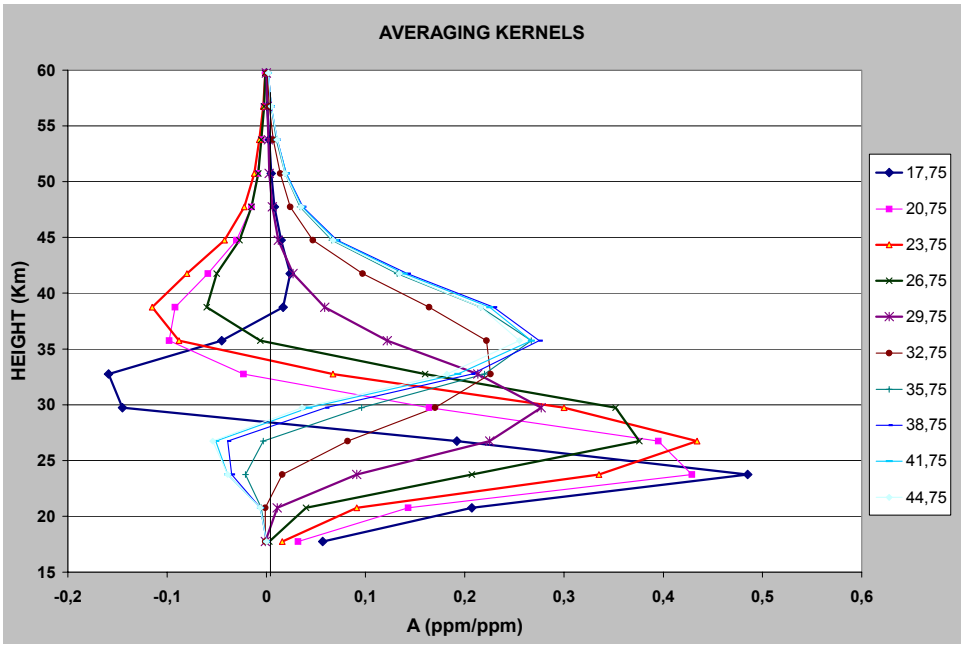

Figure 2: Averaging kernels of the retrieval process.

Eq. (14), is used to compare measurements (in our case TROPWA data) with other measurements or model calculation with much higher resolution and then much less dependence on the a priori (in our case HALOE data). The high resolution case can be considered as "ideal case", and then eq. (14) can be written as[10]:

$$\mathbf{x}_s = \mathbf{x}_a + \mathbf{A}(\mathbf{x}_h - \mathbf{x}_a) \tag{17}$$

where $\boldsymbol{x}_s$ is the smoothed version of the higher resolution profile. However, when analyzing relative variations of measurements given by the same instrument, this error is not considered, because it is constant for those measurements. Figure 4 shows the contribution functions (matrix **D**, eq. 12), indicating how much a 1 K noise in a given channel of the spectrometer influences the inversion process. For example, the black line with "x" represents the weight that 1 K additive noise has in the retrieved profile for the 60 MHz channel.

The overall error calculation (eq. 7) give us the final covariance, that is, the foreseen uncertainties for each height, including all factors that can affect the retrieval procedure (errors in the inversion process, errors due to the a-priori profiles, errors due to noise in the information, etc.). Summarizing, the error sources can be divided in two main categories: the statistical errors and the systematic errors, and can be calculated as seen above. For our instrument, the statistical sources, which are the tropospheric attenuation and measurement noise (integration time), resulted into an uncertainty of 3 to 7% for the tropospheric attenuation, while less than 1% for the measurement noise. Systematic error arises from sideband suppression and residual baseline structures, leading a 3 to 5% uncertainty;

calibration uncertainties reach 1 to 2 %. These uncertainties yield into relative errors of about 7-10% (0.25 - 0.7 ppm) between 15 and 20 km, up to 11% from 20 to 25 km (0.8 – 1.1 ppm) and about 6-8 % (0.5 – 0.7 ppm) from 30 to 45 km.

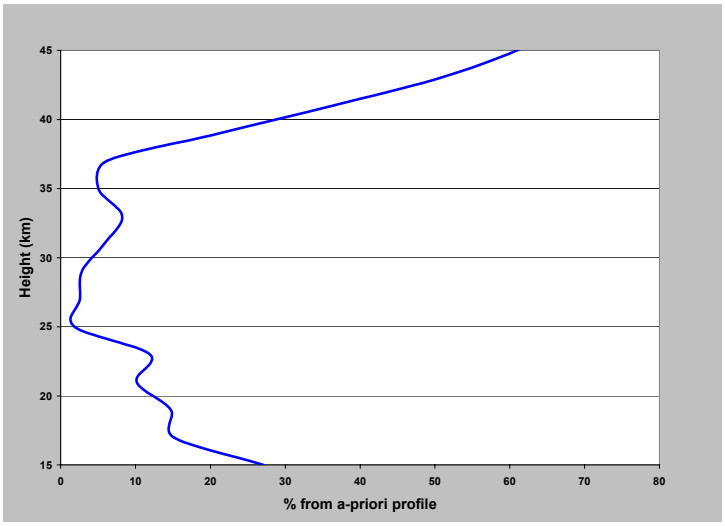

Figure 3: Influence of the a-priori information

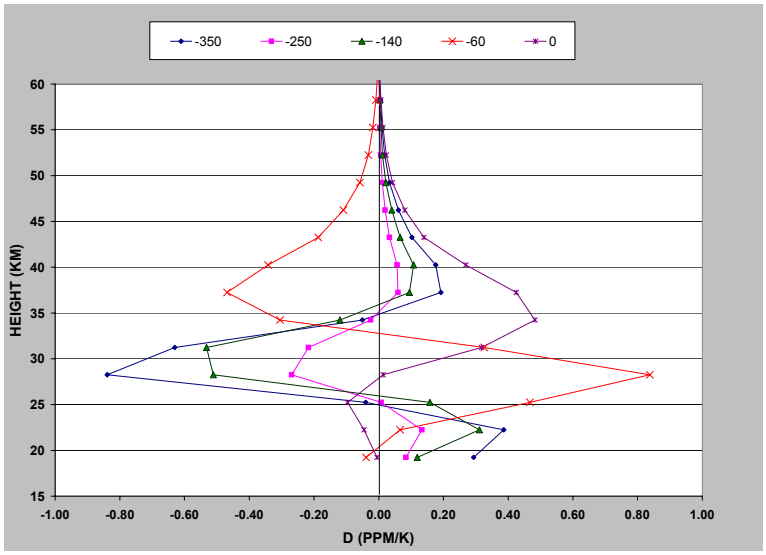

Fig. 4: Contribution functions for the TROPWA Project

3 RESULTS

3.1. Ground based stratospheric ozone measurements from 1993 – 2000

As a result of this project, ozone radiometric measurements were obtained from 1993 to 2000. From these data base, 1820 - 10 minutes - brightness temperature spectra were selected, which in turn generated 303 - 2h integration time - ozone profiles, distributed in 60 days. Table 1 resumes the temporal distribution of these ozone profiles. Bimonthly average profiles were calculated using all available profiles for that particular period, for the 8 years time span. Figure 5 shows this averaged ozone profiles, while figure 6 illustrates the uncertainties in the ozone profiles versus the atmospheric height, reaching a relative accuracy from 7 to 11% depending on the altitude, month of the year, and measurement site, according the above described error analysis. Figure 7 shows the resulting stratospheric ozone profiles retrieved during this period

3.2. HALOE stratospheric ozone measurements over Mendoza from 1993 – 2000

In order to compare our results, we selected 83 stratospheric ozone profiles measured by the HALOE instrument[12] over the Mendoza region (33° S, 68 W), within the period 1993 – 2000. As coincidence criterion, the ozone HALOE profiles were chosen not more than +/- 5° away from Mendoza latitude and at most +/- 10 ° in longitude. The average profiles resulted in mean latitude of 34.37 S and a mean longitude of 67.68 W with a mean deviation of 3.5° in latitude and 4.5° in longitude. HALOE measurements for the Mendoza region are obtained, in average, around once per month (considering sunset and sunrise profiles). Figure 8 show the selected 83 HALOE ozone profiles for the Mendoza region.

In the comparison process, it must be taken into account the different geographical and temporal view of the selected profiles. Additionally, the HALOE ozone profiles have a higher vertical resolution in contrast to the TROPWA measurements. As said above in the discussion of the averaging kernels, and eq. (16), retrievals from ground based radiometry, as TROPWA instruments, uses the pressure broadening information to derive the altitude dependence of the ozone emission, therefore they have a coarser vertical resolution compared to the HALOE profiles. For this reason, the HALOE ozone profiles were averaged, by convolving them with the averaging kernels of the lower resolution TROPWA instrument. Comparative studies[11] among different instruments have used similar coincidence criterion and also used the averaging kernels for comparing results.

As an example of the degree of coincidence, we present bimonthly average profiles from HALOE and TROPWA instruments, at the period 1993 –2000 for the area above Mendoza. The averaged HALOE profiles are shown in fig. 9, while figure 10 depicts the relative differences between both instruments.

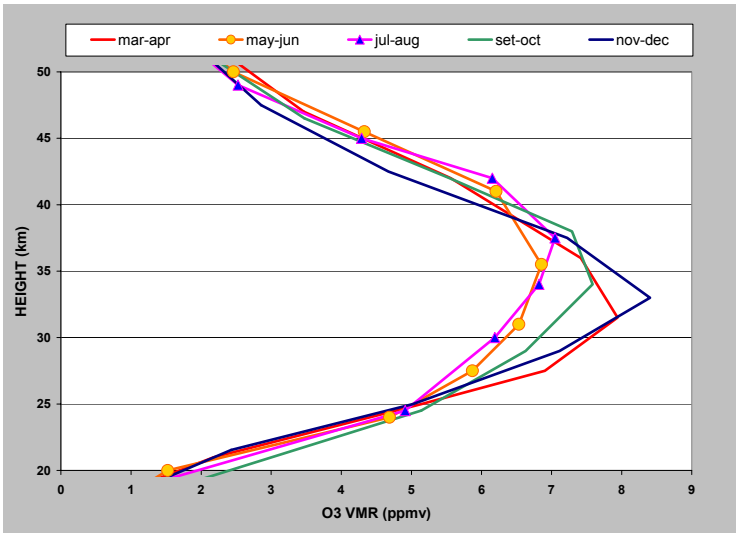

Figure 5: TROPWA bi-monthly ozone profiles over Mendoza, from years 1993 to 2000.

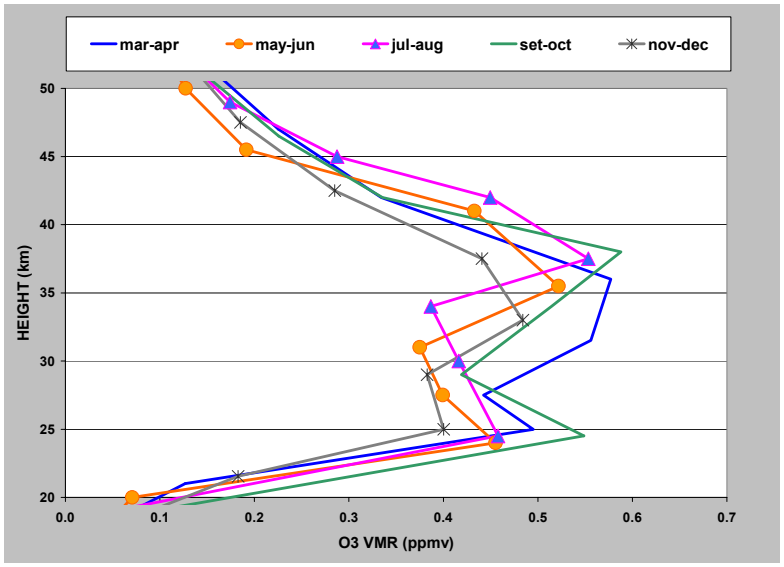

Figure 6: Relative errors calculated for the averaged ozone profiles (fig. 5).

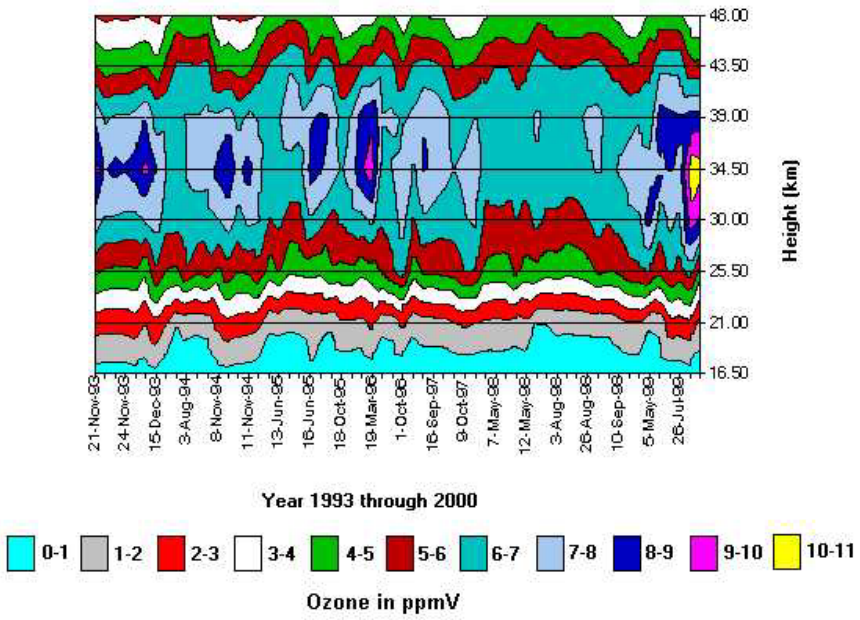

Figure 7: TROPWA Ozone Profiles over Mendoza, years 1993-2000

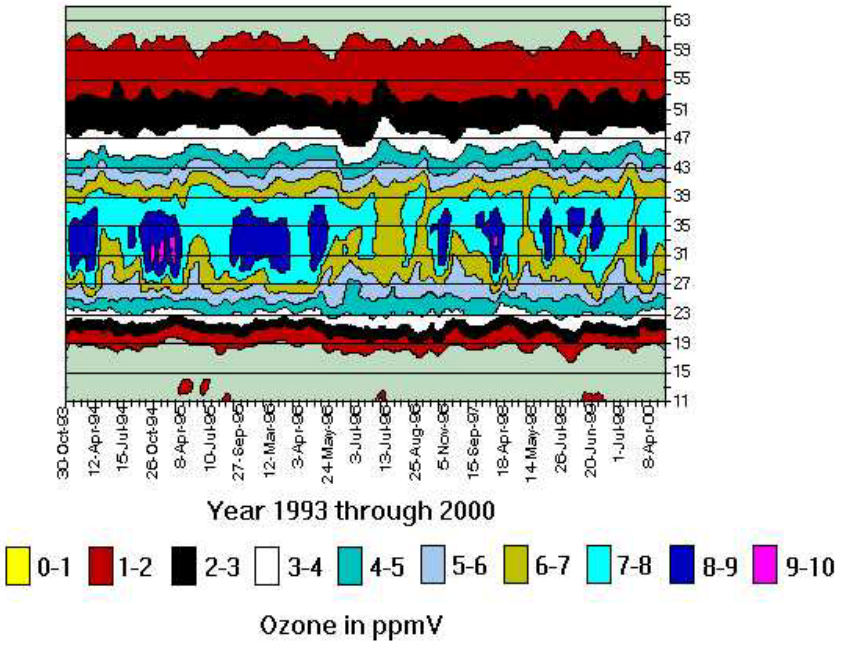

Figure 8: HALOE Ozone Profiles over Mendoza, years 1993-2000

In these figures we show the convolved HALOE profiles. Comparing these measurements, a difference between + 0.4 to - 0.8 ppmv (about + 8 to –10 %) in the period of May-June between both profiles can be observed. The major difference occurs, normally, for the maximum profile value, i.e., around 35 km height, which shows a systematic lower values for the TROPWA profiles. These differences partially arise from the influence of the TROPWA averaging kernel on the different a priori profiles selected.
Based on the error analysis of the TROPWA retrieval process, and the comparison with other instruments it can be concluded that the TROPWA instrument can retrieve profiles satisfactorily within +/- 10 % above 20 km and below 40 km.

4 CONCLUSIONS

From 1993 to 2000, the Institute for Environmental Studies (IEMA) depending of the University of Mendoza, carried out ground-based stratospheric ozone measurements by means of millimetre wave radiometry. In this project also tropospheric water vapour was measured to characterize the tropospheric attenuation affecting the ozone measurements.

To evaluate and validate the stratospheric ozone profiles retrieved from the TROPWA measurements, a theoretical error analysis is presented followed by comparative study using the HALOE ozone profiles. This study includes a comparison of individual profiles and of seasonal averages from 1993 to 2000. We selected 60 daily profiles from TROPWA and 83 profiles from HALOE over Mendoza, with a coincidence criterion of +/- 5° in latitude and at most +/- 10 ° in longitude. The average profiles resulted in mean latitude of 34.37 S and a mean longitude of 67.68 W with a mean deviation of 3.5° in latitude and 4.5° in longitude.

These coincident HALOE measurements for the Mendoza region correspond approximately to one profile per month. Given the coarser height resolution of the retrieved ozone profiles from microwave ground based instrument, compared to those obtained from the solar occultation technique, the HALOE profiles were averaged by convolving them with the averaging kernels of the TROPWA retrieval process. This error analysis and the comparison tests allowed us to evaluate and characterize the retrieval of our instrument. It can be seen that from 20 to 40 km the TROPWA instrument is able to retrieve ozone profiles with absolute errors varying from 10 to 20 %, and relative errors less than 5%, with a height resolution (FWHM) that varies from 5 to 11 km depending on the altitude. The seasonal variations show consistent patterns but having TROPWA measurements a systematic lower peak value of about 0.5 to 0.7 ppmv. The mayor discrepancies between both set of profiles occurs in the period of May-June with values varying around +8 to –10% (+0.4 to –0.8 ppmv). This difference is partially due to the coarser height resolution of our instrument.

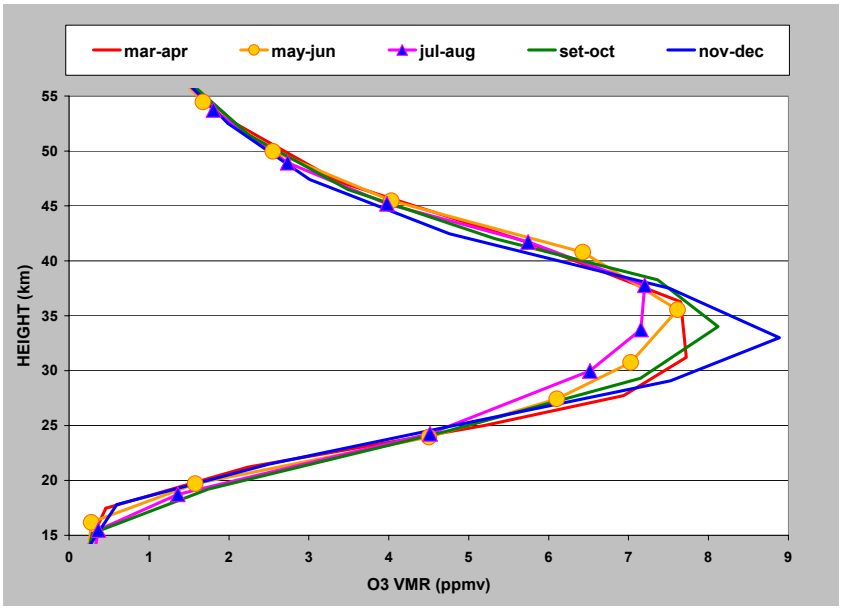

Figure 9: Averaged HALOE bi-monthly profiles.

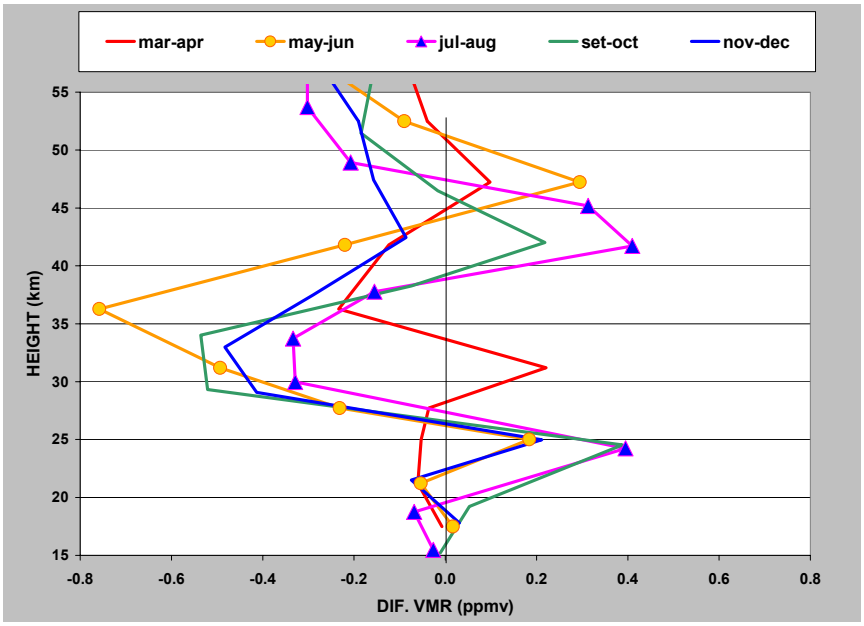

Figure 10: Differences between TROPWA and HALOE bi-monthly profiles.

5 ACKNOWLEDGEMENTS

The authors wish to thank the authorities of the University of Mendoza and the Max-Planck Institut für Aeronomie for their support to this research activity. We also thank the HALOE Project and the MAS Project for the public availability of the data. The Argentine National Weather Service is here acknowledged for kindly permitting the use of the radiosounding data.

6 REFERENCES

[1] Russell, J. M., Gordley, L. L., Park, J. H., Drayson, S.R., Hesketh, W. D., Cicerone, R. J., Tuck, A. G., Frederick, J. E., Harrries, J.E., and Crutzen, P. J.: "The Halogen Occultation Experiment". *Journal of Geophysical Research*, 98, 10777-10797.

[2] Brühl, C., Drayson, S. R., Russell III, J. M., Crutzen, P. J., McInerney, J., Purcell, P. N., Claude, H., Gernand, H., McGee, T., McDermid, I. and Gunson, M. R.: "HALOE Ozone Channel Validation". *Journal of Geophysical Research,* 101, 10,217-10,240, (1996).

[3] Chandrasekhar, S.: "*Radiative Transfer*". Dover Publications, Inc., New York, (1960).

[4] Ulaby, F. T., Moore, R. K., Fung, A. K.: "*Microwave remote sensing. Active and Passive*". Artech House Inc.(1981).

[5] Puliafito, C., Puliafito, E., Hartmann, G., Quero, J.L.: "Determination of stratospheric ozone profiles and tropospheric water vapor content by means of microwave radiometry". *Proceedings of the VIII Simpósio Brasileiro de Microondas e Óptica (SBMO 98*), Joinville - SC, Brasil, 274-278, (1998).

[6] Rodgers, C.D.: "Retrieval of atmospheric temperature and composition from remote measurements of thermal radiation". *Rev. Geophys.,* 14, 609-624*,* (1976).

[7] Puliafito, S.E., Bevilacqua, R., Olivero, J., Degenhardt: W.: "Retrieval error comparison for several inversion techniques used in limb-scannig millimeter wave spectroscopy". *Journal of Geophysical Research,* 100, 14,257 - 14,268, (1995).

[8] Rodgers, C.D.: "Characterization and error analyses of profiles retrieved from remote sounding measurements", *Journal of Geophysical Research,* 95, 5587-5595. (1990).

[9] Nedoluha, G., Bevilacqua, R.M., Gomez, R.M., Thacker, D.L., Waltman, W.B. , Pauls, T.: "Ground-based measurements of water vapor in the middle atmosphere", *Journal of Geophysical Research*, 100, D2, 2927-2939, (1995).

[10] Rodgers, C.D. and Connor, B.: "Intercomparison of remote sounding instruments" *Journal of Geophysical Research,* 108, D3, 4116, ACH13 , 1 – 14, (2003).

[11] Nedoluha, G.E., Bevilacqua, R.M., Gomez, R.M. , Waltman, W.B., Hicks, B.C. , Thacker, D.L., Russell III, J.M., Abrams, M., Pumphrey, H.C., Connor, B.J.: "A Comparative Study of Mesospheric Water Vapor Measurements from the Ground Based Water Vapor Millimeter Wave Spectrometer and Space Based Instruments". *Journal of Geophysical Research*, 102, 16647-16661, (1997).

[12] NASA-HALOE web site: http:\\haloedata.larc.nasa.gov\home.html.